NO-REFERENCE IMAGE QUALITY ASSESSMENT METRIC BY COMBINING FREE ENERGY THEORY AND STRUCTURAL DEGRADATION MODEL

Ke Gu[1,2]*, Guangtao Zhai*[1,2]*, Xiaokang Yang*[1,2]*, Wenjun Zhang*[1,2]*, and Longfei Liang*[3]

[1]Institute of Image Communication and Information Processing, Shanghai Jiao Tong University, Shanghai, China
[2]Shanghai Key Laboratory of Digital Media Processing and Transmissions
[3]Bocom Smart Network Technologies Inc.

ABSTRACT

In the research of image quality assessment (IQA), no-reference approaches are usually thought of as a big challenge since none of original image information is available. To tackle this problem, we propose a new no-reference image quality metric through combining two recently proposed reduced-reference IQA models, namely the free energy based distortion metric (FEDM) and the structural degradation model (SDM). In this work, it will be shown that there exists an approximate linear relationship between the original image information of the free energy feature and the structural degradation information. Based on this observation and the application of support vector machine (SVM) that is widely used in the current study of IQA, our newly developed No-reference Free energy and Structural degradation based Distortion Metric (NFSDM) is found to alleviate the dependance of original images, and has achieved remarkably well prediction accuracy, outperforming the most two full-reference IQA approaches PSNR/SSIM and several mainstream no-reference image quality metrics.

Index Terms— Image quality assessment (IQA), no-reference (NR), free energy, structural degradation, human visual system (HVS)

1. INTRODUCTION

The task of image quality assessment (IQA), mainly consisting of subjective and objective assessment, is an important research area in digital image processing. Although the subjective assessment method should be the terminal quality criterion, it is very expensive, time-consuming, and not practical for real-time image processing systems. As a result, an increasing number of researchers have devoted to objective IQA metrics during the last decade. Following the tremendous achievement of SSIM [1], it has been acknowledged that structural information plays a significant role in the research of IQA. Since then, many improved SSIM-type of IQA metrics have been developed and obtained higher prediction performance as full-reference (FR) IQA metrics, such as MS-SSIM [2], IW-SSIM [3], S_NW-SSIM [4], SC-SSIM [5] and DIP [6].

Nowadays, the study of no-reference (NR) IQA algorithms is in the stage of booming evolution. Generally speaking, there are two types of NR image quality metrics. The first type of no-reference methods aim to detect some specific artifacts. In the earlier attempts of IQA approaches, a blind blur metric [7] was proposed based on the analysis of the spread of the edges in image. For JPEG compression, Wang *et al* [8] developed a method through measuring blocking effects and relative blur that contains average absolute difference between in-block image samples and zero-crossing rate. Recently, the scale invariant based noise estimator (SINE) [9] was exploited for white noise injection.

The second type of no-reference approaches depend on some features extracted by statistic models (e.g. natural scene statistics (NSS) model) in transform domains. For example, Sheikh *et al* [10] employed the NSS model to assess the quality of JPEG2000 compressed images. Later, BLind Image Integrity Notator using DCT Statistics (BLIINDS-II) [11] was developed using the NSS model for DCT coefficients. In addition, wavelet transform domain-based Blind Image Quality Indices (BIQI) [12] and Distortion Identification-based Image Verity and INtegrity Evaluation (DIIVINE) [13] also relied on the NSS model. All of those methods conform to a two-stage framework, namely distortion identification followed by distortion-specific quality assessment.

Besides above-mentioned two types of NR methods, recently proposed no-reference free energy based quality metric (NFEQM) [14] belongs to a novel type of no-reference IQA algorithm. NFEQM was designed by resorting to psychovisual theories of the human visual system (HVS), and was shown to be able to accurately assess the qualities of images that are distorted by Gaussian blur or white noise injection.

In this paper, we will explore a new group of image features for NR IQA, by combining the structural degradation information and the free energy feature. In the structural degradation model (SDM) [15], structural degradation information was proposed based on an observation, which tells that images with various distortion types and quality levels, when being post-processed by low-pass filtering, will have different degrees of loss in spatial frequency. The free energy de-

fined in [14] can be estimated by measuring the gap between a viewing scene and the corresponding brain's prediction using the internal generative model. In our research, it was noticed that structural degradation information is closely related to the free energy. More specifically, the structural degradation and free energy has a proximate linear relationship for original images. Considering the fact that the reduced-reference SDM and FEDM metrics are based on highly correlated image features, we believe their partial information for the original image can be alleviated, and the integration of structural degradation information and free energy feature are capable of predicting the image quality in the no-reference condition. And meanwhile, inspired by mainstream NR methods, such as BLIINDS-II [11] and DIIVINE [13], we also take the support vector machine (SVM) [16] in account. Accordingly, this paper proposes a new No-reference Free energy and Structural degradation Distortion Metric (NFSDM).

The rest of this paper is organized as follows. Section 2 first presents the definition of extracted features of free energy and structural degradation information. Then, by combining both of them, we propose the NFSDM algorithm. In Section 3, experimental results using the LIVE database [17] are reported and analyzed. Finally, Section 4 concludes this paper.

2. THE PREDICTION MODEL

Generally, the state of the art NR image quality metrics make use of extracted features in transform domains. However, we found that the structural degradation information and free energy theory can offer another group of effective features. Thus, this paper develops the framework of the proposed NFSDM metric by a nonlinear combination of two parts of features, free energy and structural degradation information, as illustrated in Fig. 1.

2.1. Free energy feature

The underlying idea of FEDM metric [14] is mainly based on the free energy principle, which is proposed by Friston [18]-[19] to explain and unify several brain theories in biological and physical sciences about human action, perception and learning. Nearly to the Bayesian brain hypothesis, a basic premise of the free energy based brain theory is that the cognitive process is manipulated by an internal generative model. Using the generative model, human brain renders predictions of those encountered scenes in a constructive manner.

This constructive model is a probabilistic model in essential, which can decompose into a likelihood term and a prior term. Then, visual perception is the process of inverting this likelihood term so as to infer the posterior possibilities of the given scene. Not surprisingly, there always exists a gap between the encountered scene and brain's prediction, due to the fact that the internal generative model cannot be universal. The gap between the external input and its generative-model-explainable part can be directly related to the quality of perceptions, and therefore measures the image quality.

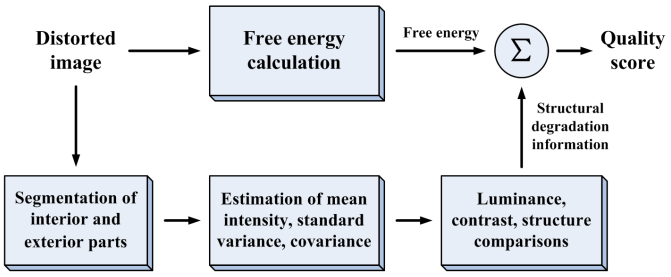

Fig. 1. The primary framework of the proposed NFSDM algorithm.

For operational amenability, it is assumed that the internal generative model $\mathcal{G}$ for visual perception is parametric, which explains perceived scenes by adjusting the vector $\boldsymbol{\theta}$ of parameters. Given an image, its 'surprise' (determined by entropy) can be evaluated by integrating the joint distribution $P(I, \boldsymbol{\theta}|\mathcal{G})$ over the space of model parameters $\boldsymbol{\theta}$

$$-\log P(I|\mathcal{G}) = -\log \int P(I, \boldsymbol{\theta}|\mathcal{G}) d\boldsymbol{\theta}. \tag{1}$$

By introducing an auxiliary term $Q(\boldsymbol{\theta}|I)$ into both the denominator and numerator in Eq. (1) and it can be rewritten as

$$-\log P(I|\mathcal{G}) = -\log \int Q(\boldsymbol{\theta}|I) \frac{P(I, \boldsymbol{\theta}|\mathcal{G})}{Q(\boldsymbol{\theta}|I)} d\boldsymbol{\theta}. \tag{2}$$

Then, through using Jensens inequality, it can be obtained from Eq. (2):

$$-\log P(I|\mathcal{G}) \leq -\log \int Q(\boldsymbol{\theta}|I) \frac{P(I, \boldsymbol{\theta})}{Q(\boldsymbol{\theta}|I)} d\boldsymbol{\theta}, \tag{3}$$

and the right hand side, as the definition of free energy:

$$J(\boldsymbol{\theta}) = -\log \int Q(\boldsymbol{\theta}|I) \frac{P(I, \boldsymbol{\theta})}{Q(\boldsymbol{\theta}|I)} d\boldsymbol{\theta}. \tag{4}$$

Finally, the free energy feature of a distorted image Y can be defined as $J(\hat{\boldsymbol{\theta}}_Y)$ with $\hat{\boldsymbol{\theta}}_Y = \arg\min J(\boldsymbol{\theta}|\mathcal{G}, Y)$. More details can be found in [14].

2.2. Structural degradation information

In our previous work [15], it was noticed that for most images with various distortion categories and quality ranks, their blurred version that is processed by low-pass filtering will have different degrees of spatial frequency decrease. This observation reveals one big shortcoming of SSIM, which lacks of adequate ability to distinguish different distortion types and quality levels. So, an improved structural degradation information is developed as follows.

Referring to the definitions of μ_Y and σ_Y in SSIM, we redefine $\mu_Y(d)$ and $\sigma_Y(d)$ for simulating Gaussian low-pass filters with different coefficients:

$$\mu_Y(d) = \frac{1}{N^2}\sum_{i=1}^{N}\sum_{j=1}^{N} w_{ij}y_{ij}$$
$$\sigma_Y(d) = \sqrt{\frac{\sum_{i=1}^{N}\sum_{j=1}^{N} w_{ij}(y_{ij}-\mu_Y(d))^2}{N^2-1}} \quad (5)$$

with $\mathbf{w} = \{w_{ij}|i,j = 1,\ldots,N\}$, satisfying $Sum(\mathbf{w}) = 1$ and $Var(\mathbf{w}) = d$ ($Sum(\cdot)$ and $Var(\cdot)$ are used to compute the sum and variance values independently).

Then, by selecting different variance d (= 0.1 and 1.5), the degrees of spatial frequency decrease for a distorted image Y can be estimated as structural degradation information:

$$SD_{m_c,t,N}(Y) = \frac{2\cdot\mu_{Y1}\cdot\mu_{Y2}+C_1}{\mu_{Y1}^2+\mu_{Y2}^2+C_1}$$
$$SD_{m_s,t,N}(Y) = \frac{\sigma_{\mu_{Y1}\mu_{Y2}}+C_3}{\sigma_{\mu_{Y1}}\sigma_{\mu_{Y2}}+C_3}$$
$$SD_{v_s,t,N}(Y) = \frac{\sigma_{(\sigma_{Y1}\sigma_{Y2})}+C_3}{\sigma_{\sigma_{Y1}}\sigma_{\sigma_{Y2}}+C_3} \quad (6)$$

where $\sigma_{(\sigma_{Y1}\sigma_{Y2})}$ refers to the definition of $\sigma_{(AB)}$:

$$\sigma_{(AB)}(d) = \frac{\sum_{i=1}^{N}\sum_{j=1}^{N} w_{ij}(a_{ij}-\mu_A(d))(b_{ij}-\mu_B(d))}{N-1} \quad (7)$$

and

$$\mu_{Y1} = \mu_Y(d=0.1) \quad \mu_{Y2} = \mu_Y(d=1.5)$$
$$\sigma_{Y1} = \sigma_Y(d=0.1) \quad \sigma_{Y2} = \sigma_Y(d=1.5) \quad (8)$$

and $t = \{i, e\}$ for interior parts or exterior parts of blocks. As can be seen from Fig. 2, for a block with the size of 8×8, the dark gray part are the exterior part, while the middle part colored with light gray are the interior part.

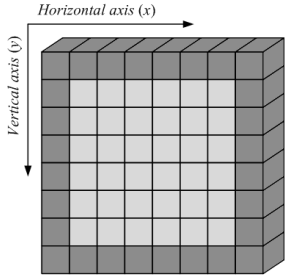

Fig. 2. Illustration of interior parts or exterior parts of blocks. For a block with the size of 8×8, the dark gray part are the exterior part, while the middle part colored with light gray are the interior part.

2.3. SVM based nonlinear combination

To better explain why the information of original images can be eliminated, we still need to define the free energy and structural degradation information of an original image X as $J(\hat{\boldsymbol{\theta}}_X)$ (with $\hat{\boldsymbol{\theta}}_X = \arg\min J(\boldsymbol{\theta}|\mathcal{G}, X)$) and $SD_{s,t,N}(X)$ (with $s = \{m_c, m_s, v_s\}$) according to Eq. (4), (6). We then compare the results of free energy and structural degradation information for original images. Fig. 3 illustrates there exists an approximate linear relationship between $J(\hat{\boldsymbol{\theta}}_X)$ and $SD_{s,t,N}(X)$, and Table 1 presents a group of approximate values satisfying

$$J(\hat{\boldsymbol{\theta}}_X) = \alpha_s \cdot SD_{s,t,N}(X) + \beta_s, \quad (9)$$

which can provide a possible opportunity to avoid original image information through using an effectively nonlinear combination.

Table 1. Different groups of α and β values approximating the linear relationship between $J(\hat{\boldsymbol{\theta}}_X)$ and $SD_{s,t,N}(X)$.

	$SD_{m_c,t,N}(X)$	$SD_{m_s,t,N}(X)$	$SD_{v_s,t,N}(X)$
α	-8.994	-9.643	-4.416
β	11.88	12.34	6.700

Enlightened by recently proposed no-reference methods (BLIINDS-II and DIIVINE) that have powerful performance in predicting image quality scores, it has become a mainstream methodology to make use of SVM for regression. It is well-known that SVM performs well in high-dimensional spaces. And moreover, it can validly avoid over-fitting and have good generalization capabilities. So this paper adopts SVM to train the chosen features and predict quality scores for all the distortions. The total number of features used in our work is 55, mainly consisting of two groups. The first group includes only one, namely free energy values of distorted images. The other gourd involves 54 features, which can be easily obtained. Considering the fact that the scale factor has important effects on the study of IQA, such as MS-SSIM [2] and SAST [20], we also takes into account various scales by introducing scale factor $f = 2, 4, 8, 16$ for interior parts and $f = 2, 4$ for exterior parts. In general, the energy recited by human eyes has a lower bound. When the local region is very complicated, different sizes of windows used to generate Gaussian blur filters should be applied, i.e., we set $N = 3, 7, 11$ in Eq. 5. Here, we still condenser using $\widehat{SD}_{s,t,N,f}(Y) = J(\hat{\boldsymbol{\theta}}_Y) - (\alpha_s \cdot SD_{s,t,N,f}(Y) + \beta_s)$ to alleviate as much original information as possible. In summary, the selected features are shown as follows:

$$\begin{cases} J(\hat{\boldsymbol{\theta}}_Y) & \text{with } \hat{\boldsymbol{\theta}}_Y = \arg\min J(\boldsymbol{\theta}|\mathcal{G}, Y) \\ \widehat{SD}_{s,i,N,f}(Y) & \text{with } s=\{m_c, m_s, v_s\}, \\ & \quad N=\{3,7,11\}, f=\{2,4,8,16\} \\ \widehat{SD}_{s,e,N,f}(Y) & \text{with } s=\{m_c, m_s, v_s\}, \\ & \quad N=\{3,7,11\}, f=\{2,4\} \end{cases} . \quad (10)$$

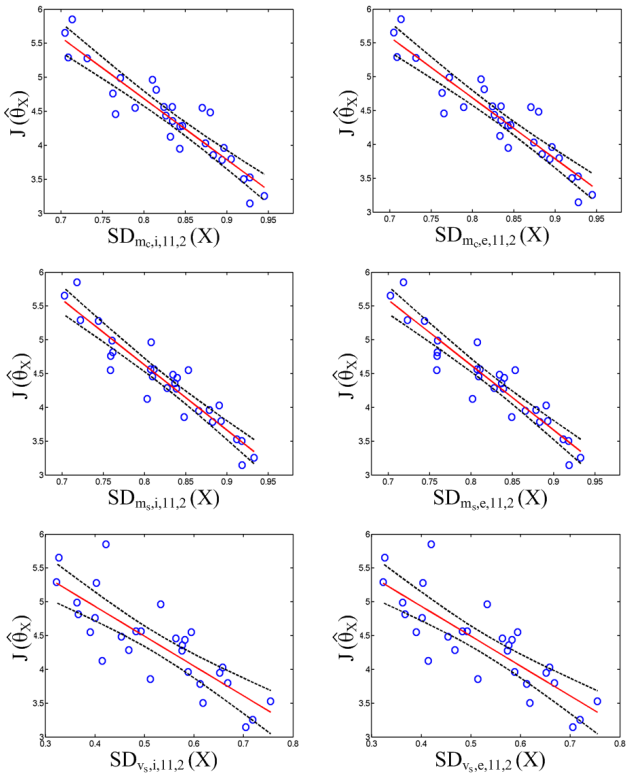

Fig. 3. Scatter plots of $J(\hat{\boldsymbol{\theta}}_X)$ vs. $SD_{s,t,N,f}(X)$ ($s = \{m_c, m_s, v_s\}$, $t = \{i, e\}$, $N = 11$, $f = 2$) for 29 original images in LIVE database. The (red) lines are the fitted straight lines and the (black) dash lines are 95% confidence intervals.

Note, the relationship of objective results versus subjective scores are completely different between images of white noise and other distortion categories, such as FEDM and SDM. To illustrate, the higher-quality white noise images have larger FEDM or SDM values, while other distortion categories of images with lower quality correspond to smaller FEDM or SDM results. Consequently, the $\widehat{SD}_{s,t,N,f}(Y)$ is further modified as follows:

$$\widehat{SD}_{s,t,N,f}(Y) = \begin{cases} -\widehat{SD}_{s,t,N,f}(Y) & \text{if } J(\hat{\boldsymbol{\theta}}_Y) > 5 \\ \widehat{SD}_{s,t,N,f}(Y) & \text{otherwise} \end{cases}. \quad (11)$$

We then employ SVM to train the 55 features in terms of differential mean opinion scores (DMOSs). In this work, the LIVE database [17], consisting of 29 reference images and 779 distorted images, is utilized as the testing bed for verify the performance of our NFSDM metric. Similar to the usual training method, the training set contains about 80% of the reference images and their corresponding distorted versions, while the testing set consists of the rest 20% of the reference images and their associated distorted images. In order to ensure that the proposed approach is robust across content and is not governed by the specific train-test split, this paper reuses this random 80% train - 20% test split 1000 times on the LIVE dataset, and evaluate the performance on each of these test sets.

3. EXPERIMENTAL RESULTS

Three commonly used performance metrics, Pearson Linear Correlation Coefficient (PLCC), Spearman Rank-Order Correlation Coefficient (SROCC) and Root Mean-Squared Error (RMSE) as suggested by VQEG [21], are employed to further evaluate our superior NFSDM algorithm and the other nine methods, namely PSNR, SSIM, Pina [7], Wang [8], SINE [9], Sheikh [10], NFEQM [14], BLIINDS-II, and DIIVINE on the LIVE database. First of all, Fig. 4 shows the scatter plots of DMOS versus the best performance of NFSDM on five different data sets of distortion categories and the whole LIVE database.

Secondly, Table 2 compares the overall performance of all the aforementioned NR image quality metrics. Obviously,

Table 2. Pearson Linear Correlation Coefficient (PLCC), Spearman Rank-Order Correlation Coefficient (SROCC), and Root Mean-Squared Error (RMSE) values (after nonlinear regression) of PSNR, SSIM, BLIINDS-II, DIIVINE, and the proposed NFSDM method (NFSDM (m) and NFSDM (o) are the median value and the optimal value across 1000 times training) on the whole LIVE database (779 images).

Algorithm	PLCC	SROCC	RMSE
PSNR	0.8701	0.8755	13.475
SSIM	0.9014	0.9103	13.475
BLIINDS-II	0.9144	0.9115	11.834
DIIVINE	0.8443	0.8560	14.649
NFSDM (m)	0.9237	0.9224	10.466
NFSDM (o)	0.9278	0.9270	10.194

Table 3. Pearson Linear Correlation Coefficient (PLCC) values (after nonlinear regression) of PSNR, SSIM, Pina [7], Wang [8], SINE [9], Sheikh [10], NFEQM [14], BLIINDS-II, DIIVINE and the proposed NFSDM method (NFSDM (m) and NFSDM (o) are the median value and the optimal value across 1000 times training) on five various distortion types of data sets.

Pearson Linear Correlation Coefficient (PLCC)					
Algorithm	JP2K	JPEG	WN	Gblur	FF
PSNR	0.8996	0.8878	0.9860	0.7834	0.8895
SSIM	0.9410	0.9504	0.9697	0.8743	0.9428
Pina [7]	–	–	–	0.9194	–
Wang [8]	–	0.9201	–	–	–
SINE [9]	–	–	0.9760	–	–
Sheikh [10]	0.9628	–	–	–	–
NFEQM [14]	–	–	0.9712	0.8921	–
BLIINDS-II	0.9352	0.9471	0.9653	0.9175	0.8453
DIIVINE	0.9267	0.8041	0.9914	0.9600	0.8741
NFSDM (m)	0.9550	0.9592	0.9352	0.9449	0.8480
NFSDM (o)	0.9639	0.9655	0.9305	0.9456	0.8575

Table 4. Spearman Rank-Order Correlation Coefficient (SROCC) values (after nonlinear regression) of PSNR, SSIM, Pina [7], Wang [8], SINE [9], Sheikh [10], NFEQM [14], BLIINDS-II, DIIVINE and the proposed NFSDM method (NFSDM (m) and NFSDM (o) are the median value and the optimal value across 1000 times training) on five various distortion types of data sets.

Spearman Rank-Order Correlation Coefficient (SROCC)					
Algorithm	JP2K	JPEG	WN	Gblur	FF
PSNR	0.8954	0.8809	0.9857	0.7823	0.8907
SSIM	0.9355	0.9449	0.9625	0.8944	0.9413
Pina [7]	–	–	–	0.9015	–
Wang [8]	–	0.9130	–	–	–
SINE [9]	–	–	0.9814	–	–
Sheikh [10]	0.9628	–	–	–	–
NFEQM [14]	–	–	0.9691	0.8845	–
BLIINDS-II	0.9299	0.9471	0.9594	0.9103	0.8348
DIIVINE	0.9185	0.8141	0.9878	0.9581	0.8586
NFSDM (m)	0.9506	0.9481	0.9265	0.9347	0.8205
NFSDM (o)	0.9592	0.9546	0.9172	0.9336	0.8291

Table 5. Root Mean-Squared Error (RMSE) values (after nonlinear regression) of PSNR, SSIM, Pina [7], Wang [8], SINE [9], Sheikh [10], NFEQM [14], BLIINDS-II, DIIVINE and the proposed NFSDM method (NFSDM (m) and NFSDM (o) are the median value and the optimal value across 1000 times training) on five various distortion categories of data sets.

Root Mean-Squared Error (RMSE)					
Algorithm	JP2K	JPEG	WN	Gblur	FF
PSNR	11.018	14.656	4.6660	11.479	13.015
SSIM	8.5349	9.9070	6.8453	8.9643	9.4963
Pina [7]	–	–	–	7.2666	–
Wang [8]	–	9.8804	–	–	–
SINE [9]	–	–	5.6372	–	–
Sheikh [10]	8.6076	–	–	–	–
NFEQM [14]	–	–	6.6793	8.3448	–
BLIINDS-II	8.9341	10.221	7.3153	7.3470	15.218
DIIVINE	9.4794	18.934	3.6656	5.1691	13.837
NFSDM (m)	7.4864	9.0050	9.9063	6.0445	15.098
NFSDM (o)	6.7188	8.3001	10.245	6.0118	14.657

the proposed NFSDM paradigm has achieved better results, as compared to the mainstream no-reference IQA algorithms (BLIINDS-II and DIIVINE), and the most two popular full-reference IQA methods (PSNR and SSIM). Besides, the performance of ten no-reference methods on each image dataset of five distortion types, including JPEG2000, JPEG, white noise, Gaussian blur, and fast-fading, is tabulated in Table 3-5. It can be found that our method also attains exciting results for every specific category of image distortion. For example, Table 3-5 present that, for JPEG/white noise images, the prediction accuracy of the proposed NFSDM can be comparable as that of Sheikh/SINE, the popular no-reference metrics for specific distortion type. And moreover, our algorithm has attained much better results than Pina/Wang/NFEQM when assessing quality of Gaussian blur/JPEG2000 images.

4. CONCLUSION

In this paper, we develop a novel no-reference IQA approaches NFSDM by combining features of free energy and structural degradation information. Experimental results on the LIVE database verified its remarkably well performance. First, the proposed SVM based NFSDM metric is trained for all the distortion, and it has been proved that its overall prediction accuracy is better than the mainstream no-reference IQA algorithms, such as BLIINDS-II and DIIVINE, and the most two popular full-reference PSNR and SSIM methods. Second, our method has also achieved inspiring results for each commonly specific distortion category, and can be applied to replace the classical artifact-detection based NR methods.

Besides, it needs to emphasize that our paradigm successfully constructs a bridge between the newly proposed free energy theory and early exploited structural information (structural degradation information is virtually a kind of modified structural information), so as to indicate a new direction for further comprehension of the behavior of HVS and of researches on image quality assessment.

Acknowledgment

This work was supported in part by NSERC, NSFC (61025005, 60932006, 61001145), SRFDP (20090073110022), postdoctoral foundation of China 20100480603, 201104276, postdoctoral foundation of Shanghai 11R21414200, the 111 Project (B07022), STCSM (12DZ2272600), and 2011BAK14B02.

5. REFERENCES

[1] Z. Wang, A. C. Bovik, H. R. Sheikh, and E. P. Simoncelli, "Image quality assessment: From error visibility to structural similarity," *IEEE Trans. Image Process.*, vol. 13, no. 4, pp. 600-612, April 2004.

[2] Z. Wang, E. P. Simoncelli, and A. C. Bovik, "Multi-scale structural similarity for image quality assessment," *IEEE Asilomar Conference Signals, Systems and Computers*, November 2003.

[3] Z. Wang and Q. Li, "Information content weighting for perceptual image quality assessment," *IEEE Trans. Image Process.*, vol. 20, no. 5, pp. 1185-1198, 2011.

[4] K. Gu, G. Zhai, X. Yang, L. Chen, and W. Zhang, "Nonlinear additive model based saliency map weighting strategy for image quality assessment", *IEEE International Workshop on Multimedia Signal Processing*, 2012.

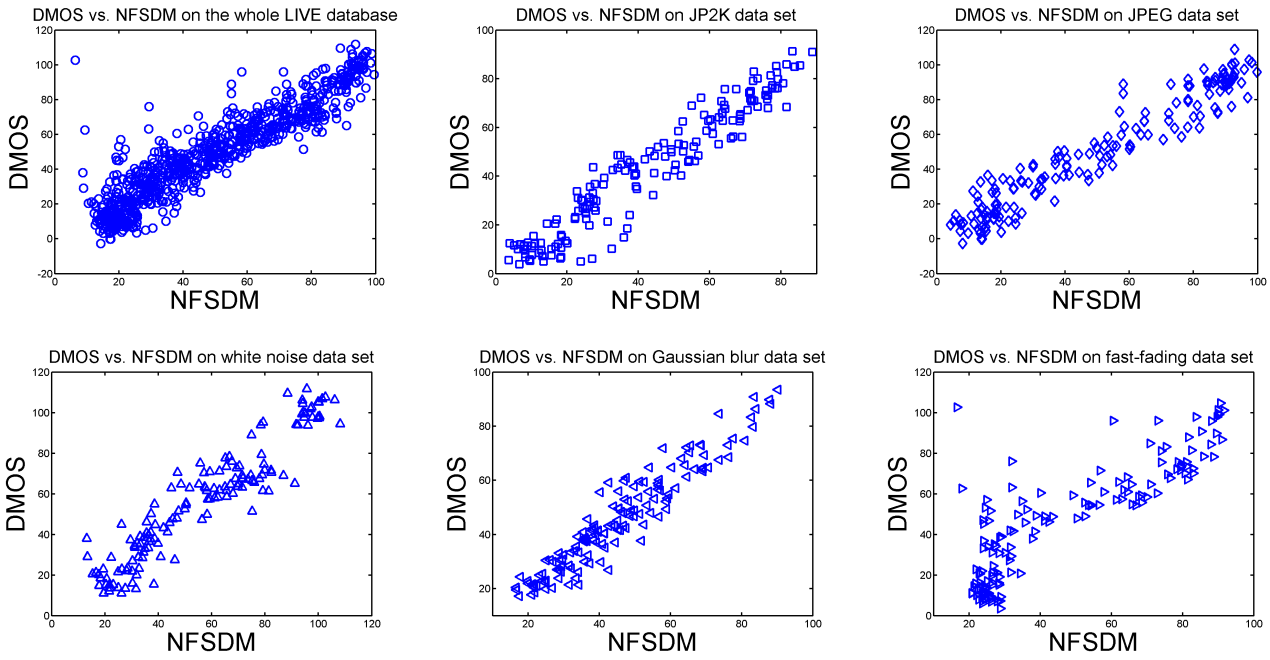

Fig. 4. Scatter plots of DMOS vs. the proposed NFSDM approach on the whole LIVE database and five different distortion types of data sets.

[5] K. Gu, G. Zhai, X. Yang, and W. Zhang, "An improved full-reference image quality metric based on structure compensation", *APSIPA ASC*, 2012.

[6] K. Gu, G. Zhai, X. Yang, and W. Zhang, "A new psychovisual paradigm for image quality assessment: from differentiating distortion types to discriminating quality conditions", *Signal, Image and Video Processing*, vol. 7, no. 3, pp. 423-436, May 2013.

[7] P. Marziliano, F. Dufaux, S. Winkler, and T. Ebrahimi, "A no-reference perceptual blur metric," *Proc. IEEE Int. Conf. Image Process.*, vol. 3, pp. 57-60, 2002.

[8] Z. Wang, H. R. Sheikh, and A. C. Bovik, "No-reference perceptual quality assessment of JPEG compressed images," *Proc. IEEE Int. Conf. Image Process.*, September 2002.

[9] D. Zoran and Y. Weiss, "Scale invariance and noise in natural images," *in Proceedings of the IEEE 12th International Conference on Computer Vision*, pp. 2209-2216, 2009.

[10] H. R. Sheikh, A. C. Bovik, and L. K. Cormack, "No-reference quality assessment using natural scene statistics: JPEG2000," *IEEE Trans. Image Process.*, vol. 14, no. 12, December 2005.

[11] M. A. Saad, A. C. Bovik, and C. Charrier, "DCT Statistics Model-based Blind Image Quality Assessment", *Proc. IEEE Int. Conf. Image Process.*, September 2011.

[12] A. K. Moorthy and A. C. Bovik, "A two-step framework for constructing blind image quality indices," *IEEE Signal Processing Letters*, pp. 587-599, vol. 17, no. 5, May 2010.

[13] A. K. Moorthy and A. C. Bovik, "Blind Image Quality Assessment: From Scene Statistics to Perceptual Quality", *IEEE Trans. Image Process.*, pp. 3350-3364, vol. 20, no. 12, December 2011.

[14] G. Zhai, X. Wu, X. Yang, W. Lin, and W. Zhang, "A psychovisual quality metric in free-energy principle," *IEEE Trans. Image Process.*, vol. 21, no. 1, pp. 41-52, January 2012.

[15] K. Gu, G. Zhai, X. Yang, and W. Zhang, "A new reduced-reference image quality assessment using structural degradation model", *Proc. IEEE International Symposium on Circuits and Systems*, 2013.

[16] C-C. Chang and C-J. Lin, "LIBSVM: a library for support vector machines," 2001, http://www.csie.ntu.edu.tw/∼cjlin/libsvm.

[17] H. R. Sheikh, Z. Wang, L. Cormack, and A. C. Bovik, "LIVE image quality assessment Database Release 2," [Online]. Available: http://live.ece.utexas.edu/research/quality.

[18] K. Friston, J. Kilner, and L. Harrison, "A free energy principle for the brain," *Journal of Physiology Paris*, vol. 100, pp. 70-87, 2006.

[19] K. Friston, "The free-energy principle: a unified brain theory?" *Nature Reviews Neuroscience*, vol. 11, pp. 127-138, 2010.

[20] K. Gu, G. Zhai, X. Yang, and W. Zhang, "Self-adaptive scale transform for IQA metric", *Proc. IEEE International Symposium on Circuits and Systems*, 2013.

[21] VQEG, "Final report from the video quality experts group on the validation of objective models of video quality assessment," March 2000, http://www.vqeg.org/.